

THREE-DIMENSIONAL AUXETIC MECHANICAL METAMATERIALS BASED ON TRIANGULAR PRISM ARCHITECTURE

A. SORRENTINO^{*} AND D. CASTAGNETTI^{*}

^{*} Dipartimento di Scienze e Metodi dell'Ingegneria (DISMI)
Università di Modena e Reggio Emilia
Via G. Amendola 2, 42122 Reggio Emilia, Italy
e-mail: andrea.sorrentino@unimore.it, davide.castagnetti@unimore.it

Abstract. Auxetic mechanical metamaterials are a class of architected materials that exhibit the exotic characteristic of a negative Poisson's ratio (NPR). This work aimed to evaluate the NPR potential of differently-oriented architected structures consisted of hinged triangular prisms connected by their corners. By implementing kinematic models of the systems, we assessed the deformation mechanism of the idealized structure: the models allow to investigate some geometrical variants of the rotating polyhedrons with different orientation schemes, which are at 45° to each other. The computational results showed that the Poisson's ratio (PR) of the system varies from -0.3 up to -1.3, depending both on geometrical parameters of the polyhedral elements and on the orientation of the unit cells. To further investigate the deformation behavior of the metamaterial, we designed prismatic architectures with chiral connections between the rotating units, which were validated using finite element (FE) method. The numerical simulations reveal a remarkably different auxetic properties between these designs, with a PR ranging between -0.08 and -0.70. Hence, physical models were additively manufactured in Onyx material and experimentally tested under uniaxial compression, showing an excellent agreement with the numerical predictions. Our results demonstrate the highly tunable NPR ability of such mechanical metamaterials, with a possible application in the biomedical field.

Key words: Auxetic Metamaterials, Hinged Models, Finite Element Analyses, Additive Manufacturing, Experimental Characterization.

1 INTRODUCTION

In this work, we investigate the anisotropic auxetic ability of polyhedral mechanical metamaterials consisted of triangular prism elements connected by their corners. Mechanical metamaterials, also known as architected materials, are artificial materials and engineered structures possessing the potential to exhibit a variety of anomalous mechanical characteristics, which are primarily attributed to their peculiar architecture rather than their material composition [1]–[3]. The unique characteristics of such mechanical metamaterials can be

obtained by rationally design the elementary cells composing the system, that gives rise to the desired macro-scale elastic properties, which are not commonly found in natural materials [4], [5]. The geometrically programmable properties of architected materials have generated enormous interest worldwide, thanks also to the advances in the field of additive manufacturing (AM), i.e. three-dimensional (3D) printing, which allow the design of novel engineered materials with unprecedented functionalities and “negative” characteristics, including a negative Poisson’s ratio (NPR) [6], [7].

NPR systems, referred to as auxetic mechanical metamaterials, feature the counter-intuitive property of contract in transverse direction upon the application of a uniaxial compression and *vice-versa*, which is a scale-independent property [8]–[10]. The negative deformation mode in auxetics promotes additional enhanced mechanical functionalities, such as increased shear modulus, synclastic curvature behavior and higher energy absorption capabilities, with applications in acoustics, textiles, electronics, and particularly, in biomechanics [11]–[13]. According to literature, NPR materials comprise 2D/3D structural motifs like as foams, honeycombs, re-entrant structures, folding systems, origami, chiral models and rotating semi-rigid architectures [6], [10].

Rotating mechanisms, namely hinged systems, represent a class of auxetic metamaterials consisted of idealized solid units connected by their corners, in which the NPR potential of the system is determined by the rotation of the rigid blocks around their vertices/joints [14], [15]. A typical example of 2D hinged motif is the rotating squares mechanism which possesses a Poisson’s ratio (PR) equal to -1 [16]. Auxeticity can be achieved from other arrangements of polygonal elements, including rectangles, triangles, rhombi and parallelograms [17], [18]. By analogy, 3D auxetic frameworks can be designed by considering prismatic geometries such as cuboids, tetrahedrons and polyhedral units, including some variants of them with chiral connections between the rotating elements, that have been shown to manifest an anisotropic NPR behavior [19]–[23]. However, despite the number of works in the field of rotating models, the multi-axial performance of these types of structures were not consistently studied, even by considering different types of connectivity and loading regimes [24]–[27].

In this context, the work presents a class of differently-oriented mechanical metamaterials containing hinged triangular prisms and analyzed their auxetic characteristic. Through kinematic models of the architected material, the work firstly examines some peculiar configurations of the hinged structure by varying the geometrical dimensions and the orientation of the elementary cells. The kinematic results reveal the highly anisotropic auxetic behavior of these systems, with a PR that vary between -0.3 and 1.3 over significant strange ranges. Secondly, we designed and additively manufactured two geometrically-related architected structures in polymeric material, which were characterized by chiral ligaments between the rotating units. The deformation behavior of these designs was investigated using finite element (FE) models and experimentally validated by performing experimental tests. FE results revealing a good correlation with the experiments, thus obtaining metamaterial architectures with a wide range of PR, depending of type of orientation scheme considered. Thanks to their programmable mechanical properties and functionalities, the proposed architected models represent a valid alternative for the design of novel biomedical metamaterials for bone substitute implants.

2 PRISMATIC ARCHITECTURES

Figure 1 presents geometrically-related architected materials with prismatic unit cells, which structural motif is based on the metamaterial model recently proposed by the same authors [23].

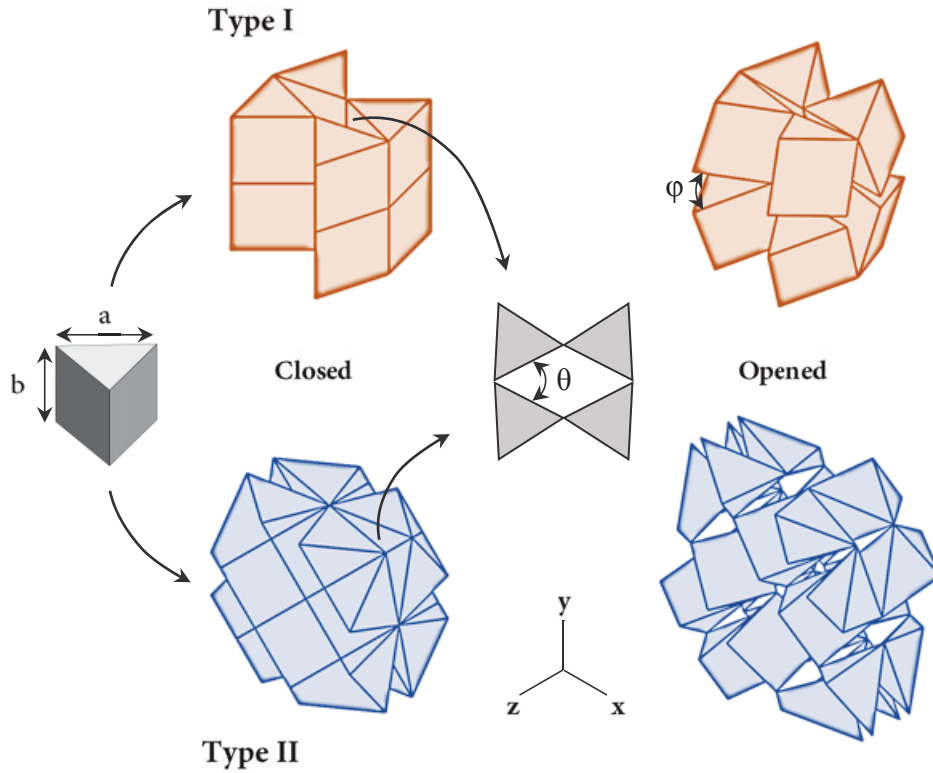


Figure 1: RUCs of the two differently-oriented architected materials investigated, namely *Type I* and *Type II*, in their undeformed (closed) and deformed (opened) configurations. Details on geometrical parameters of the prismatic elements were also provided in the Figure.

As shown in Figure 1, the elementary unit of the systems comprise triangular prism elements connected by ideal hinges at their corners, whose geometrical dimensions are described by the length, a , and the height of the prism, b . The two idealized models depicted in Figure 1, namely *Type I* and *Type II* architectures, were initially considered “closed”, such that, the orientation between the polyhedral elements is identified by their internal angle, denoted as θ . In more detail, *Type I* model resembling the typical form of the metamaterial structure with triangular prisms reported in [23], while *Type II* architecture represents a variant of the former, which is rotated at 45° along the z - direction of the system. Hence, the representative unit cells (RUCs) of such materials are distinctly different. In order to construct metamaterial models with different orientation schemes, we designed architected structures where the projection of the RUC in the x - y plane identifies a quadratic shape when the system is fully compressed (i.e. when closed), even if the prismatic elements are rotated at 45° as in *Type II* architecture.

According to these considerations, the geometric condition necessary to construct the metamaterial schemes in Figure 1 is the following:

$$b = a \cos(\vartheta/2) \quad (1)$$

Thus, the deformation of these structures results from the tilting of the solid elements around their vertices, i.e. the pivoted corners, upon the application of a uniaxial tensile displacement along the nodes (and/or faces) on two opposite edges, depending whether type model considered. This tilting of the prisms causes void spaces in the structures, which leads to the final open configurations of the metamaterials depicted in Figure 1, suggesting a NPR behavior in all directions, where φ represents the characteristic angle of the structures. The next section investigates through quantitative kinematic analyses the auxetic abilities of these idealized models.

3 HINGED STRUCTURES

3.1 Computational models

To predict the deformation behavior of the hinged architectures with solid units, we implemented kinematic models of the structures using the CAD/CAE software *Solidworks* [28]. Specifically, the computational models describe the prisms as rigid bodies and the hinges at their vertices as ideal (i.e. frictionless), thus, the Young's modulus of the structure is equal to zero. The analyses applied periodic boundary conditions (PBCs) to the RUC of the systems, thus simulated the architected materials as infinite systems. In brevity, periodicity of the RUC entails that all pairs of opposite boundary nodes (/surfaces) of the simulated structure under a given loading regime deform identically. Hence, the internal pivoted corners of the systems were coupled with the adjacent vertices of the attached rotating prisms. Details on the method are provided elsewhere [23].

In order to investigate the auxeticity of the metamaterials, we performed a numerical analysis plan by varying the internal angle of the structure, θ (see Figure 1), from 10° to 60° in steps of 10° . Then, the model applied a tensile displacement in the y - direction on the top and bottom nodes (and/or faces) of the RUCs, corresponding to a metamaterial configuration that is fully-opened. However, for all the simulated structures, the side length of the prisms, a , was set equal to 1 mm , for which, the value of b/a of the structure varies from 0.996 to 0.866, see Figure 1.

By examining the displacement field predicted by the computational models, we calculated the strains by considering the variation of the apparent volume of the structure, and estimated the PRs of the systems in three principal directions, namely v_{yx} , v_{yz} , v_{zx} .

3.2 Hinged structure results

Figure 2.A shows the deformation behavior of *Type I* and *Type II* hinged models with θ equal to 60° , along the frontal plane of the system, namely the yx plane. Additionally, Figure 2.B presents the variation of the PRs of the metamaterial architectures in all the principal directions

upon the changing of the characteristic angle, namely φ .

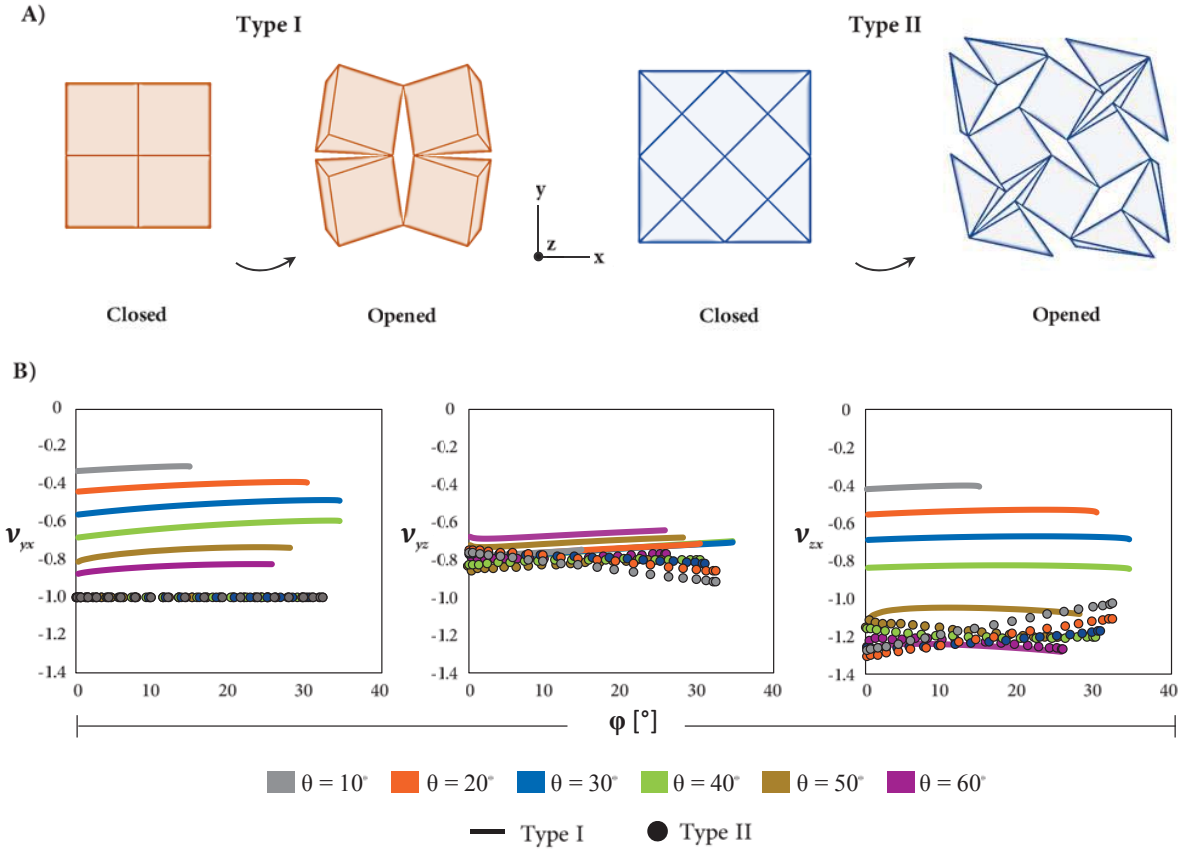


Figure 2: Kinematic model results: undeformed (closed) and deformed (opened) configurations of *Type I* and *Type II* systems with θ equal to 60° (A). Evolution of PRs of the hinged models with variation of internal angle θ , and characteristic angle φ , upon the principal directions of the structure (B).

4 CHIRAL SYSTEMS

4.1 Design and finite element analyses

In this section, we designed and analyzed chiral architectures resembling the structural shape of the hinged materials presented above. The designed architectures were constructed using the same CAD software used for the kinematic analysis. According to the numerical results in Figure 2.B, we focused on *Type I* and *Type II* models with θ equal to 30° . Specifically, we introduced chiral ligaments with circular cross-section area between the solid units, thus obtaining architected materials that feature a tetra-chiral topology [29], see Figure 3.A. The geometrical parameters of the unit cell of the system are: the length, l , and the diameter, d , of the chiral connections, and the height, h , of the prismatic nodes, which were chosen equal to 10 mm, 3 mm and 14.5 mm, respectively. Additionally, we fillet the edges of each polyhedron,

which prevents localized stress concentration phenomena [30]. The chiral cells depicted in Figure 3.A were used to construct a $2 \times 2 \times 2$ RUCs of the systems, resulted in cubic architectures showed in Figure 3.B. Then, we simulated the *quasi-static* compression behavior of these designs through 3D finite element (FE) models using the implicit solver of *Abaqus* [31]. For all the simulated metamaterials, we discretized the structure using second-order tetrahedral elements, where the side length of each element was set equal to 0.6 mm . The material used is Onyx[®], a micro carbon filled polyamide. Specifically, an isotropic elasto-plastic material model was used for the meshes, with a Young's modulus, E_m , of 605 MPa , and a Poisson's ratio, ν_m , of 0.34 , where the yield stress of the polymer, σ_y , is equal to 13.9 MPa . Therefore, the analysis involved nonlinearity. To simulate the compressive behavior of the systems, we imposed boundary conditions to the structures. First, we constrained all the nodes of the bottom surfaces of the metamaterials. Second, the structures were axially compressed by applying a vertical displacement to the top surfaces of the systems, up to a value of global axial strain equal to 5% . Hence, we calculated the elastic modulus of the metamaterials, E_y , according to [20]. We determined the PR of structure, ν_{yx} , by evaluating the strains field of the central RUC of the metamaterial model, Figure 3.C, at the maximum value of the applied strain (for further details see [23]). Additionally, the FE analyses provided the Maximum Principal stress of the simulated models.

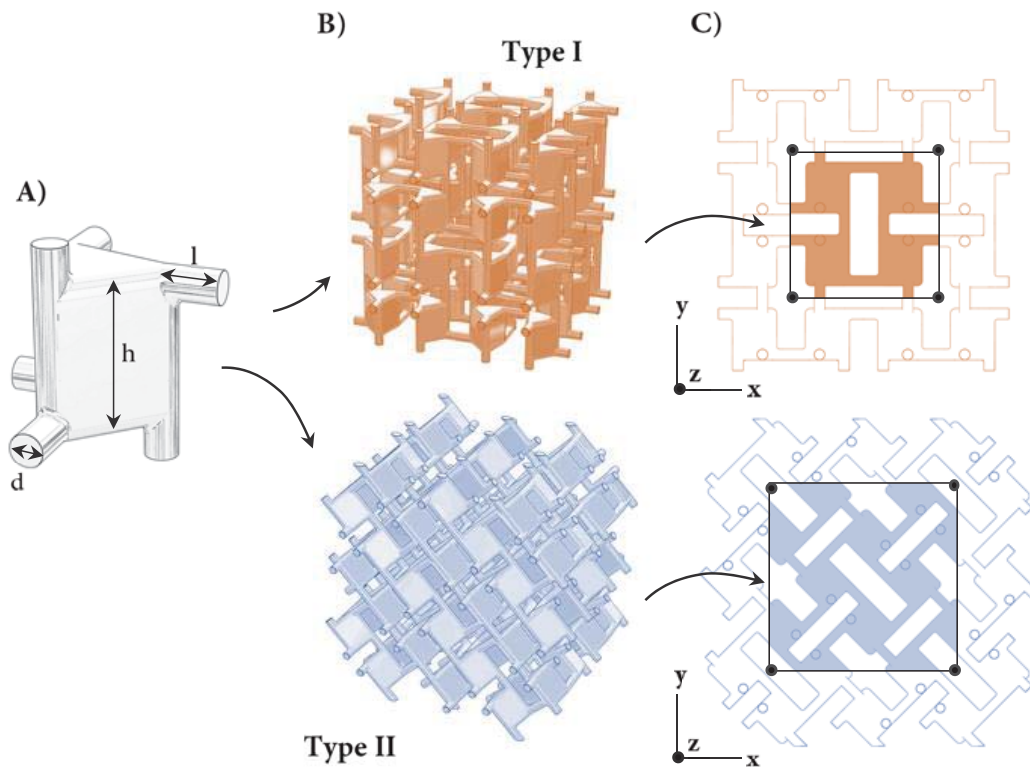


Figure 3: Chiral unit cell (A). *Type I* and *Type II* chiral designs (B) with highlighted central RUC of the systems used for calculating the PR along the yx plane of the metamaterials (C).

4.2 Prototypes development and experimental characterization

To validate the FE simulations, we additively manufactured and tested the designed chiral architecture presented in Section 4.1. Physical models were built on a fused filament fabrication *Markforged* 3D printer using the Onyx[®] material, and optimized the printing parameters to ensure high quality prototypes, Figure 4. Briefly, we considered a 35% infill density with a hexagonal pattern and a layer thickness equal to 0.2 mm. The prototypes have relative density between 0.16% and 0.19%, with a maximum transversal dimension of 92 mm for *Type II* architecture. The specimens were axially compressed using a *Galdabini* SUN 550 testing machine, up to a final displacement corresponding to an overall global strain of the prototypes equal to 5%, which is identical to those applied in the FE models. The elastic modulus of the systems, E_y , was calculated according to the standard [32]. To estimate the PR of the metamaterials, we measured the displacement components of the central RUC in the front surface of the systems by using a high resolution digital camera. Strains were obtained through image post-processing in *Matlab*, by tracking the voids surrounding the central RUC of the sample (see Figure 3.C), and then used to calculate the local average PR of the structures, ν_{yx} (for detail see [23], [33]).

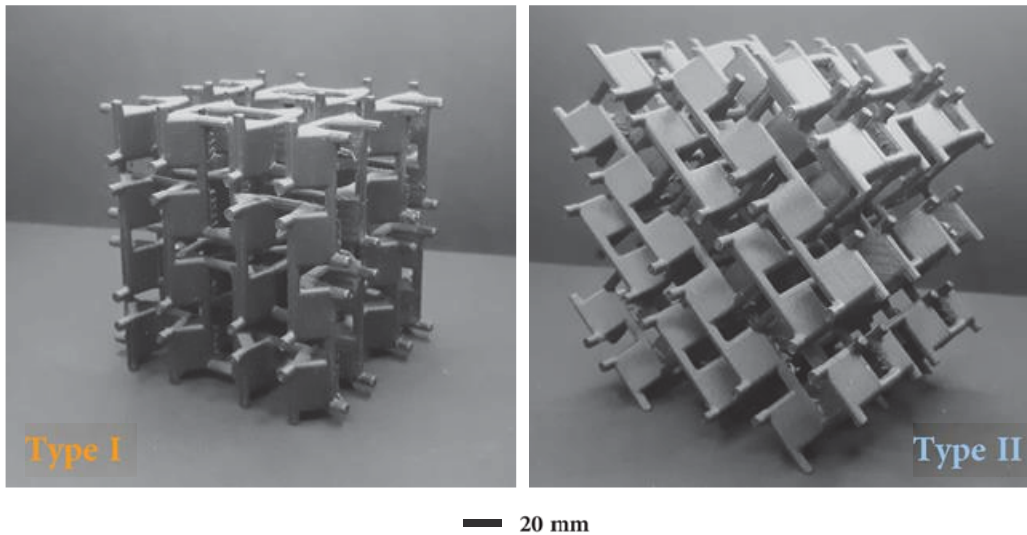


Figure 4: Additively manufactured prototypes of the chiral metamaterial designs investigated.

4.3 Chiral system results

Figure 5.A compares the numerical and the experimental deformation behavior of the investigated materials, while Figure 5.B shows the Maximum Principal stress contour acting on the structures, evaluated for global axial strain of the system equal to 5%. Finally, Table 1 reports the main elastic properties of the chiral designs according to numerical simulations with those retrieved from the experiments.

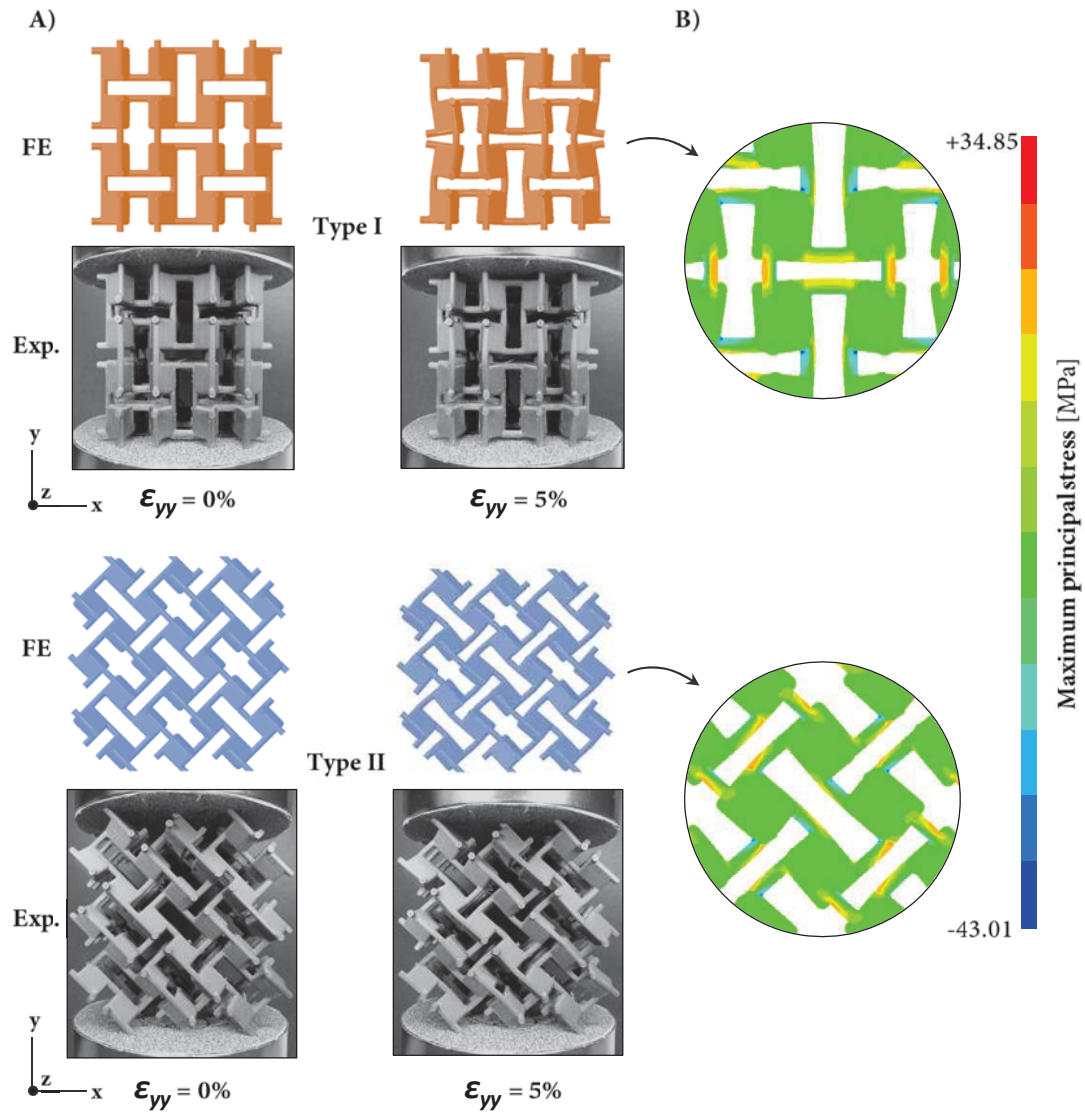


Figure 5: Comparison between the FE and experimental deformation behavior of the chiral designs investigated (A). Maximum principal stress contour in the central RUC structures for global axial strain equal to 5% (B).

Table 1: Numerical and experimental mechanical properties of the chiral metamaterials.

	ν_{yx}		E_y / E_m [%]	
	Exp.	FE	Exp.	FE
Type I	-0.67	-0.70	0.26	0.23
Type II	-0.11	-0.08	0.14	0.16

5 DISCUSSION

From the kinematic results of Figure 2.A, it is clearly evident that both the hinged models manifested a negative Poisson's ratio property, since the tilting of the solids units leads to increase the voids in the structure, and consequently, to increase the apparent volume of the metamaterial. However, the *Type II* architecture exhibits a strongly auxetic effects, testified by the relative higher size of voids in the system respect to its non-rotated counterpart. As emerged from Figure 2.B, all the architected models were characterized by a significantly anisotropic auxetic behavior, which is more predominant in *Type I* materials. Specifically, in *Type I* materials, the value of ν_{yx} becomes more negative by increase the value of angle θ , with a minimum PR of -0.82; whilst reaches a constant value of -1 for all *Type II* designs. On the other hand, the trend of ν_{yz} is more complex, which, for *Type II* models, is less negative for geometrical architectures with θ equal to 50° and 60° , with a similar trend observed also for the *Type II* configurations. Hence, viewed in the zx plane, the variations of ν_{zx} for *Type I* models have a similar performance to those observed for ν_{yx} , with a minimum of -1.28 for the architecture with lower angle θ . Moreover, the *Type II* metamaterial with maximum θ , possesses the ability of reaching the same value of PR manifested by its geometrical related counterpart. On the whole, the values of PR are nearly constant over significant strain ranges.

Therefore, the variation of the structural motif in the metamaterial design, especially by the introduction of chiral ligaments between the solid prisms, have an enormous effect in the mechanical properties and deformation behavior of these materials. As depicted in Figure 5.A, the two representative systems showed remarkably different deformation behavior and auxetic abilities. In particular, the *Type I* chiral model retains their NPR characteristic: this auxetic behavior is very similar for both numerical prediction and experiments. On the other hand, as illustrated in Figure 5.A, the *Type II* design manifested a strongly different deformation behavior respect to its idealized model, showing a large reduction in auxeticity, with an excellent qualitative agreement between the FE model and the experimental tests. This is probably the result of the relative higher length of ligaments, since this modification in the auxeticity is typically observed for rotating unit models with chiral characteristics subject to off-axis loading regimes [26], [34]. As we expected, the peak of stresses in the metamaterials are primarily located at the joint's regions of the systems, see Figure 5.B, where *Type I* architecture exhibits the highest level of stress intensity, particularly, along the vertical ligaments between the rotating units.

As reported in Table 1, in *Type I* metamaterial model, the value of numerical PR was equal to -0.70, with a very close agreement to those obtained from the experimental tests. On the other hand, for the *Type II* design, the numerical ν_{yx} assumes a value of -0.08, in accordance to those extracted from the experimental results, which value is equal to -0.11. Moreover, the results in Table 1 indicates that the value of the normalized elastic modulus in *Type I* model is about twice of one of *Type II*, with a good agreement between the FE predictions and the experiments.

Although the engineering approach here presented represents a valuable route for the design of novel architected materials, the multi-axial mechanical response of these chiral metamaterials is yet to be fully investigated. Moreover, it could be noticed that the designed metamaterials could potentially extend the range of PR of classical prismatic auxetic solids,

useful, for example, in the design and fabrication of new meta-biomaterials for AM-ed orthopedic implants [35].

6 CONCLUSIONS

The present work proposed, designed and validated a class of geometrically-related mechanical metamaterials consisted of triangular prism elements connected by the corners, which possess the ability to exhibit a negative Poisson's ratio (NPR) behavior. There are three main steps of this work: kinematic simulations, numerical analyses and experimental validation. Kinematic models investigated different geometrical configurations of the idealized hinged systems, showed that the NPR of the system vary upon the change of orientation of the unit cells as well by varying the geometrical parameters of the prismatic elements. Based on this structural motif, chiral architectures were designed and analyzed using finite element (FE) method. Hence, physical models were additively manufactured and experimentally validated, thus yielded metamaterial architectures with a wide range of Poisson's ratio, which were characterized by different elastic properties, depending of type of orientation scheme considered. Experimental results are in good correlation with those obtained from the numerical models. The work illustrates the NPR ability of such architected models, whose mechanical properties can be tailored for a specific application, provides a new paradigm for the design of 3D-printed metamaterial for the biomedical field.

REFERENCES

- [1] M. Benedetti, A. du Plessis, R. O. Ritchie, M. Dallago, S. M. J. Razavi, and F. Berto, "Architected cellular materials: A review on their mechanical properties towards fatigue-tolerant design and fabrication," *Materials Science and Engineering R: Reports*, vol. 144, p. 100606, 2021.
- [2] J. U. Surjadi *et al.*, "Mechanical Metamaterials and Their Engineering Applications," *Advanced Engineering Materials*, vol. 21, no. 3, p. 1800864, 2019.
- [3] X. Yu, J. Zhou, H. Liang, Z. Jiang, and L. Wu, "Mechanical metamaterials associated with stiffness, rigidity and compressibility: A brief review," *Progress in Materials Science*, vol. 94, pp. 114–173, 2018.
- [4] A. A. Zadpoor, "Mechanical meta-materials," *Materials Horizons*, vol. 3, no. 5, pp. 371–381, 2016.
- [5] L. J. Gibson and M. F. Ashby, "The mechanics cellular materials of three-dimensional cellular materials," *Proc. R. Soc. Lond*, vol. A382, pp. 43–59, 1982.
- [6] E. Barchiesi, M. Spagnuolo, and L. Placidi, "Mechanical metamaterials: a state of the art," *Mathematics and Mechanics of Solids*, vol. 24, no. 1, pp. 212–234, 2019.
- [7] X. Zhou *et al.*, "Advances in 3D/4D printing of mechanical metamaterials: From manufacturing to applications," *Composites Part B: Engineering*, vol. 254, p. 110585, 2023.
- [8] R. Lakes, "Foam Structures with a Negative Poisson's Ratio," *Science*, vol. 235, no.

- 4792, pp. 1038–1040, 1987.
- [9] R. S. Lakes, “Negative-Poisson’s-Ratio Materials: Auxetic Solids,” *Annual Review of Materials Research*, vol. 47, no. February, pp. 63–81, 2017.
- [10] T.-C. Lim, *Mechanics of Metamaterials with Negative Parameters*. 2020.
- [11] Y. K. Gao, “Auxetic metamaterials and structures,” *Cailiao Gongcheng/Journal of Materials Engineering*, vol. 49, no. 5, pp. 38–47, 2021.
- [12] M. Wallbanks, M. F. Khan, M. Bodaghi, A. Triantaphyllou, and A. Serjouei, “On the design workflow of auxetic metamaterials for structural applications,” *Smart Materials and Structures*, vol. 31, no. 2, 2022.
- [13] K. Bertoldi, V. Vitelli, J. Christensen, and M. van Hecke, “Flexible mechanical metamaterials,” *Nature Reviews Materials*, vol. 2, no. 11, p. 17066, 2017.
- [14] J. N. Grima, V. Zammit, R. Gatt, A. Alderson, and K. E. Evans, “Auxetic behaviour from rotating semi-rigid units,” *Physica Status Solidi (B) Basic Research*, vol. 244, no. 3, pp. 866–882, 2007.
- [15] J. N. Grima, R. Caruana-Gauci, M. R. Dudek, K. W. Wojciechowski, and R. Gatt, “Smart metamaterials with tunable auxetic and other properties,” *Smart Materials and Structures*, vol. 22, no. 8, 2013.
- [16] J. N. Grima and K. E. Evans, “Auxetic behavior from rotating squares,” *Journal of Materials Science Letters*, vol. 19, no. 17, pp. 1563–1565, 2000.
- [17] J. N. Grima-Cornish, D. Attard, J. N. Grima, and K. E. Evans, “Auxetic Behavior and Other Negative Thermomechanical Properties from Rotating Rigid Units,” *Physica Status Solidi - Rapid Research Letters*, vol. 16, no. 2, pp. 1–24, 2022.
- [18] D. Attard, E. Manicaro, and J. N. Grima, “On rotating rigid parallelograms and their potential for exhibiting auxetic behaviour,” *Physica Status Solidi (B) Basic Research*, vol. 246, no. 9, pp. 2033–2044, 2009.
- [19] C. Andrade, C. S. Ha, and R. S. Lakes, “Extreme Cosserat elastic cube structure with large magnitude of negative Poisson’s ratio,” *Journal of Mechanics of Materials and Structures*, vol. 13, no. 1, pp. 93–101, 2018.
- [20] A. Sorrentino and D. Castagnetti, “Negative Poisson’s ratio lattice for designing vertebral biomaterials,” *Mechanics of Advanced Materials and Structures*, vol. 29, no. 27, pp. 6626–6633, 2022.
- [21] A. Alderson and K. E. Evans, “Rotation and dilation deformation mechanisms for auxetic behaviour in the α -cristobalite tetrahedral framework structure,” *Physics and Chemistry of Minerals*, vol. 28, no. 10, pp. 711–718, 2001.
- [22] D. Attard and J. N. Grima, “A three-dimensional rotating rigid units network exhibiting negative Poisson’s ratios,” *Physica Status Solidi (B) Basic Research*, vol. 249, no. 7, pp. 1330–1338, 2012.
- [23] A. Sorrentino and D. Castagnetti, “Novel polyhedral mechanical metamaterial exhibiting negative Poisson’s ratio,” *Smart Materials and Structures*, vol. 32, no. 3, 2023.
- [24] H. M. A. Kolken and A. A. Zadpoor, “Auxetic mechanical metamaterials,” *RSC Advances*, vol. 7, no. 9, pp. 5111–5129, 2017.
- [25] A. A. Zadpoor, “Mechanical performance of additively manufactured meta-biomaterials,” *Acta Biomaterialia*, vol. 85, pp. 41–59, 2019.

- [26] L. Mizzi, A. Sorrentino, A. Spaggiari, and D. Castagnetti, “A comparison between rotating squares and anti-tetrachiral systems: Influence of ligaments on the multi-axial mechanical response,” *Proceedings of the Institution of Mechanical Engineers, Part C: Journal of Mechanical Engineering Science*, p. 095440622110431, 2021.
- [27] A. Sorrentino, D. Castagnetti, L. Mizzi, and A. Spaggiari, “Rotating squares auxetic metamaterials with improved strain tolerance,” *Smart Materials and Structures*, vol. 30, no. 3, 2021.
- [28] S. E. Edition, “3D DESIGN AND SIMULATION Education Edition.” 2019.
- [29] W. Wu, W. Hu, G. Qian, H. Liao, X. Xu, and F. Berto, “Mechanical design and multifunctional applications of chiral mechanical metamaterials: A review,” *Materials and Design*, vol. 180, no. June, p. 107950, 2019.
- [30] A. Sorrentino, D. Castagnetti, A. Spaggiari, and E. Dragoni, “Shape optimization of the fillet under a bolt’s head,” *Journal of Strain Analysis for Engineering Design*, vol. 54, no. 4, pp. 247–253, 2019.
- [31] M. Smith, *ABAQUS/Standard User’s Manual, Version 6.9*. United States: Dassault Systèmes Simulia Corp, 2009.
- [32] BSI, “INTERNATIONAL STANDARD Mechanical testing of metals . Ductility testing . Compression test for porous and cellular metals,” vol. ISO 13314, no. 1. 2011.
- [33] K. Bertoldi, P. M. Reis, S. Willshaw, and T. Mullin, “Negative poisson’s ratio behavior induced by an elastic instability,” *Advanced Materials*, vol. 22, no. 3, pp. 361–366, 2010.
- [34] A. Sorrentino, D. Castagnetti, L. Mizzi, and A. Spaggiari, “Bio-inspired auxetic mechanical metamaterials evolved from rotating squares unit,” *Mechanics of Materials*, vol. 173, no. July, p. 104421, 2022.
- [35] H. M. A. Kolken *et al.*, “Mechanical performance of auxetic meta-biomaterials,” *Journal of the Mechanical Behavior of Biomedical Materials*, vol. 104, no. January, p. 103658, 2020.